

Fluorophore-Free Luminescent Organosilica Nanoparticles

Lin Wang,[†] M.-Carmen Estévez,[†] Meghan O'Donoghue, and Weihong Tan*

Center for Research at the Bio/Nano Interface, Department of Chemistry, Shands Cancer Center and UF Genetics Institute, and McKnight Brain Institute, University of Florida, Gainesville, Florida 32611

Received October 30, 2007. In Final Form: January 4, 2008

In this paper, we report the preparation and characterization of fluorophore-free luminescent organosilica nanoparticles (NPs) with sizes varying from 50 to 250 nm. These NPs were synthesized by the Stöber method by incorporating several organosilanes together with the silicate precursor (tetraethyl orthosilicate, TEOS) to the silica matrix. The calcination of these NPs at high temperatures (600 and 700 °C) led to fluorescent and phosphorescent properties, which proved to be highly dependent on the initial composition of the silanization mixture and the heating temperature. Further characterization of this material in terms of its structural and optical properties is reported. Although the NPs are not very bright, the lifetime measurements revealed values in the millisecond range, which makes these NPs potentially attractive as luminescent materials and for time-resolved optical spectroscopic studies and bioassays.

Introduction

Luminescent, photostable, and easily functionalized silica nanoparticles (NPs) have been widely used for biochemical sensing,¹ time-resolved fluoroimmunoassay,² *in vivo* imaging of blood vessels,³ and bioanalytical assays.⁴ These NPs are typically generated by incorporating different emission centers, such as organic/inorganic fluorophores,⁴ quantum dots,³ or lanthanides,^{1,2} into the silica matrix. Among these, rare-earth elements such as terbium-, europium-, or yttrium-incorporated silica NPs offer several advantages compared to conventional organic dyes. Specifically, they are photostable and have large Stokes shifts and narrow emission bands. In addition, their long lifetime improves the performance of time-resolved fluorescent assays (TRFs) by measuring fluorescence when all the short-lived compounds have already decayed, thus offering higher levels of sensitivity. An important characteristic of these silica NPs is the encapsulation of the molecules in the silica matrix. Nonetheless, in many cases, the incorporation of the emission centers still involves multiple processing steps and requires the use of optical materials (e.g., cadmium, fluorophores, or rare-earth elements, etc.), some of which are expensive and environmentally toxic. Moreover, problems related to the stability and reproducibility of the signal can occur. For instance, the dye-doped silica NPs can suffer from dye leakage problems, which hamper their long-term stability.⁴

Luminescent organic/inorganic hybrid sol–gel silica materials, which do not require doping, are an interesting alternative to these doped NPs, especially in terms of environmental accommodation and low manufacturing cost. These NPs are typically prepared from an alkoxy silane and a variety of organic acids that react to generate a rigid porous silicate network with a broadband luminescence.^{5–9} As a result of its porous nature, a sol–gel is expected to be unstable and thus may become a major problem

for general use. Fortunately, there are well-known alternate methodologies for the preparation of monodisperse silica NPs in the submicrometer range. These strategies usually require the presence of basic conditions for the condensation of tetraethyl orthosilicate (TEOS), via either the Stöber synthesis procedure^{10,11} or the microemulsion method.^{12–14} Thus, this strategy becomes an attractive alternative to the production of silica NPs which contain no luminophore molecules and whose photoluminescence exclusively originates from the hybrid material itself. In this context, the preparation of silica NPs with inherent fluorescent properties generated by calcinating NPs at 400 °C which incorporate different amounts of APTS has recently been reported.¹⁵ Herein, following similar NP preparation procedures as well as the microemulsion method conditions, we have expanded the factors contemplated to study the luminescent properties of these NPs and we report more unique luminescence properties (i.e., phosphorescence) under a wider range of calcination conditions. Different organosilane compounds, each with several carbon centers in their structure, were mixed with TEOS, allowing their co-condensation and polymerization under basic conditions via the Stöber synthesis route. When these NPs were calcinated at temperatures between 400 and 700 °C, they not only exhibited a fluorescence emission band between 350 and 550 nm upon UV excitation but also gave a strong phosphorescence afterglow under certain preparation conditions. Lifetime measurements showed values in the millisecond range for some of the NPs, which is particularly useful for time-resolved assays.

Experimental Section

A series of organosilica NPs were prepared following a procedure similar to that of previous reports.^{2,3,8,15} Briefly, 9.9 mL of ethanol was added to a 20 mL glass vial, along with a magnetic stir bar. DI

* To whom correspondence should be addressed. E-mail: tan@chem.ufl.edu. Telephone and Fax: 352-846-2410.

[†] These authors contributed equally to this work.

(1) Sivakumar, S.; Diamente, P. R.; van Veggel, F. C. J. M. *Chem.—Eur. J.* **2006**, *12*, 5878–5884.

(2) Ye, Z.; Tan, M.; Wang, G.; Yuan, J. J. *Mater. Chem.* **2004**, *14*, 851–856.

(3) Chan, Y.; Zimmer, J. P.; Stroh, M.; Steckel, J. S.; Jain, R. K.; Bawendi, M. G. *Adv. Mater.* **2004**, *16*, 2092–2097.

(4) Wang, L.; Wang, K.; Santra, S.; Zhao, X.; Hilliard, L. R.; Smith, J. E.; Wu, Y.; Tan, W. *Anal. Chem.* **2006**, *78*, 646A–654A.

(5) Brankova, T.; Bekiari, V.; Lianos, P. *Chem. Mater.* **2003**, *15*, 1855–1859.

(6) Carlos, L. D.; Sa Ferreira, R. A.; Pereira, R. N.; Assuncao, M.; de Zea Bermudez, V. *J. Phys. Chem. B* **2004**, *108*, 14924–14932.

(7) Green, W. H.; Le, K. P.; Grey, J.; Au, T. T.; Sailor, M. J. *Science* **1997**, *276*, 1826–1828.

(8) Qian, G.; Wang, Z.; Wang, M. J. *Fluoresc.* **2002**, *12*, 377–382.

(9) Vinod, M. P.; Vijayamohan, K. *Appl. Phys. Lett.* **1996**, *68*, 81–83.

(10) Stöber, W.; Fink, A.; Bohn, E. J. *Colloid Interface Sci.* **1968**, *26*, 62–69.

(11) Van Helden, A. K.; Jansen, J. W.; Vrij, A. J. *Colloid Interface Sci.* **1981**, *81*, 354–368.

(12) Arriagada, F. J.; Osseo-Asare, K. J. *Colloid Interface Sci.* **1999**, *211*, 210–220.

(13) Bagwe, R. P.; Yang, C.; Hilliard, L. R.; Tan, W. *Langmuir* **2004**, *20*, 8336–8342.

(14) Zhao, X.; Bagwe, R. P.; Tan, W. *Adv. Mater.* **2004**, *16*, 173–176.

(15) Jakob, A. M.; Schmedake, T. A. *Chem. Mater.* **2006**, *18*, 3173–3175.

water (1.26 mL) and 0.4 mL of concentrated ammonium hydroxide (14.8 mol/L) were added afterward. TEOS and an organosilane, such as APTS (3-aminopropyltriethoxysilane), APTMS (3-aminopropyltrimethoxysilane), phenyltriethoxysilane, 1,4-bisnaphthyltrimethoxysilane, 1-naphthyltrimethoxysilane, or 1,4-bis (triethoxysilyl)-benzene, were simultaneously added and stirred overnight. The molar ratio of TEOS and organosilanes was varied depending on the organosilane used. NPs incorporating APTS exhibited a stronger luminescence signal than those incorporating other organosilanes. Therefore, a series of APTS NPs were prepared with the molar percentage of APTS set at 3%, 7.5%, 20%, 30%, 50%, 60%, 70%, and 80%. These spheres were washed with ethanol and DI water and then vacuum-dried and subsequently calcined in a box furnace under air at different temperatures (200, 400, 600, 700, and 800 °C) for 2 h. Calcined NPs were dissolved in DI water in an ultrasonic bath and diluted to a final concentration of 10 mg/mL. The size of the nanoparticles was around 250 nm. For the preparation of smaller nanoparticles by the Stöber method, higher amounts of both EtOH (16.75 mL) and ammonia (0.956 mL) were added with different APTS/TEOS mixtures (3.18 mmol). The obtained nanoparticles were washed and treated as described before. In the case of the microemulsion method, the particles were prepared following standard methodologies¹³ by using a quaternary mixture, with cyclohexane and hexanol as the bulk organic solvent (7.5 mL and 1.8 mL, respectively), Triton X-100 (1.77 g) as the surfactant, water (480 μ L), NH₄OH (60 μ L), and TEOS or a mixture of TEOS/APTS at different percentages to an overall amount of silane of 450 μ mol. After leaving the reaction under stirring for one night, the particles were also wash and treated as described above. Lifetime measurements were performed in a Fluorolog 322 spectrofluorometer (Jobin-Yvon, SPEX Instruments, S.A., Edison, NJ), and the data were fitted to a two-exponential decay equation. The quantum yield (QY) of the nanoparticles was determined using a comparative method using two different standard compounds (norharmane, $\lambda_{\text{ex}} = 320$ nm, λ_{em} range = 400–550 nm; quinine sulfate, $\lambda_{\text{ex}} = 350$ nm, λ_{em} range = 400–600 nm) that absorb at the excitation wavelength of choice for the sample and emit in a similar region too. Several successive dilutions of both the standards and the samples were prepared to have absorbance values at the wavelength selected below or equal to 0.1 U.A. The band pass of the excitation monochromator was set to the same values the UV–vis absorbance spectrometer used for the absorbance measurements. The UV–vis and fluorescence spectra were recorded at the fixed wavelength ($\lambda_{\text{ex}} = 350$ nm), and graphs of integrated fluorescence intensity versus absorbance were plotted. The straight line generated was used to calculate the quantum yield according to the following equation:

$$\Phi_X = \Phi_{\text{ST}}(\text{Grad}_X/\text{Grad}_{\text{ST}})(\eta_x^2/\eta_{\text{ST}}^2)$$

where the subscripts ST and X denote standard and test, respectively, Φ is the quantum yield, Grad is the gradient from the plot of integrated fluorescence intensity versus absorbance, and η is the refractive index of the solvent.

Results and Discussion

We synthesized a large range of fluorophore-free luminescent NPs. The particle size and luminescence properties were further characterized by routine spectroscopic and imaging techniques. The NP size for the standard conditions was determined to be between 200 and 250 nm using transmission electron microscopy (TEM) (see Figure 1). Smaller-sized NPs were also prepared by increasing the amount of ammonia (from 400 to 956 μ L) and the amount of EtOH (from 9.9 to 16.75 mL) following the Stöber synthesis route (leading to particles of \sim 125–150 nm) as well as the microemulsion method (with sizes around 50 nm). Both methods showed similar trends upon assessment of the final optical properties, although the photoluminescence was less intense in the microemulsion NPs (data not shown). Interestingly, incorporation of higher amounts of organosilanes did not affect

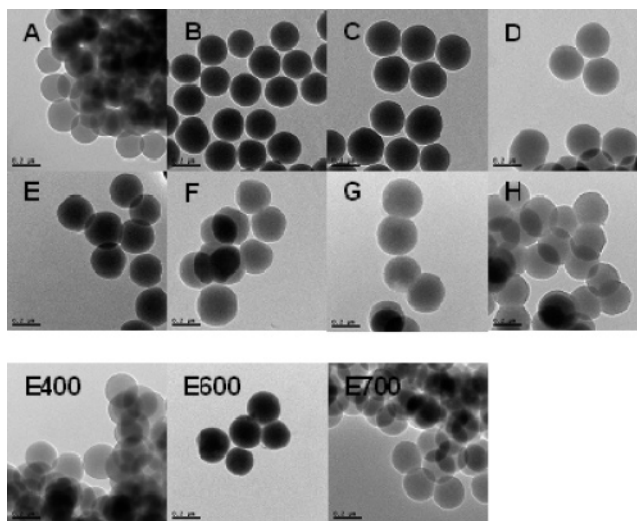


Figure 1. TEM images of NPs with different ratios of APTS before calcination at (A) 3%, (B) 7.5%, (C) 20%, (D) 30%, (E) 50%, (F) 60%, (G) 70%, and (H) 80% APTS; and after calcination at (E400) 50% APTS at 400 °C, (E600) 50% APTS at 600 °C, and (E700) 50% APTS 700 °C. The sizes of the particles are summarized in Table 1. The scale bar represents 0.2 μ m.

Table 1. Size of Luminescent Particles Prepared by the Stöber Method

NP	size (nm)	SD
3% APTS	198	14
7.5% APTS	221	12
20% APTS	259	14
30% APTS	264	10
50% APTS	251	22
60% APTS	275	15
70% APTS	264	13
80% APTS	263	22
50% APTS, 400 °C	235	13
50% APTS, 600 °C	224	15
50% APTS, 700 °C	230	10

the shape of the particles as can be seen in Figure 1. A slight decrease in size was observed in the NPs after heating, regardless of temperatures, as shown in Figure 1 and Table 1. This shrinkage could be due to progressive oxidation of the crystalline silica at higher temperatures, but, considering the inherent size dispersion, this variation could also be attributed to the synthesis method.

Interestingly, NP luminescence properties were also dependent on the heating temperature. For example, extensive heating of NPs containing gradually increasing percentages of APTS at 400 °C for 2 h changed the appearance of the powdered product from white to light tan in ambient light. Moreover, the luminescence observed under the irradiation of UV light ($\lambda_{\text{exc}} = 300$ nm) deepened, correspondingly, from light blue to yellow. Thermal treatment of these NPs at 600 °C produced pearl-colored solid materials, which exhibited light blue luminescence under UV illumination. NPs calcined at 700 °C appeared white under ambient light and blue under UV light, while no luminescence was observed after heating at 200 or 800 °C (see Figure 2). We also found that fast cooling of the NPs to room temperature or slow cooling at a rate of 5 °C/min had no effect on NP photoluminescence.

The fluorescence spectra of different solutions of the luminescent nanoparticles were recorded using a steady-state spectrofluorometer (Fluorolog TAU-3 spectrofluorometer, Jobin-Yvon, SPEX Instruments, S.A., Edison, NJ), and, from a

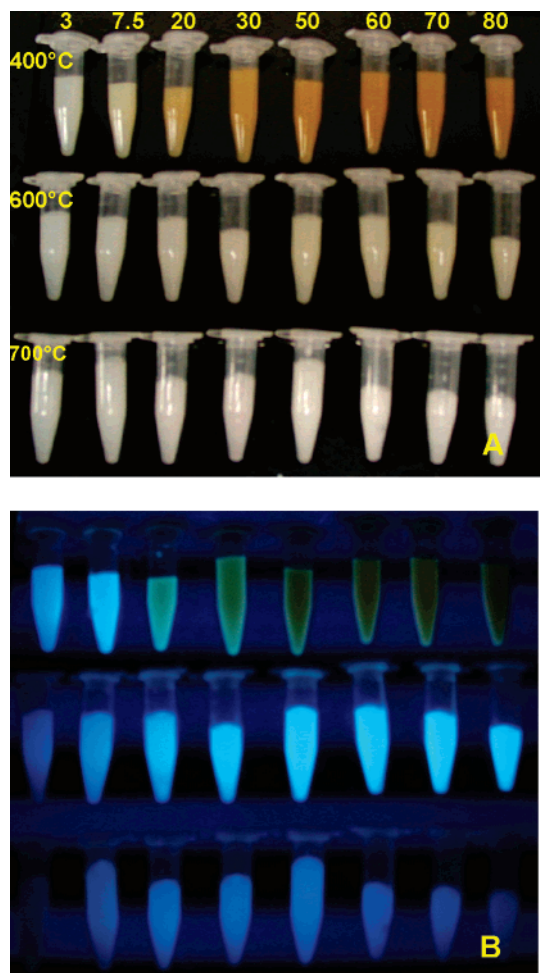


Figure 2. Images of NPs prepared with varying percentages (3–80%) of APTS and heated at different temperatures: (A) ambient light and (B) 300 nm UV illumination. The concentration of NPs is 10 mg/mL in DI water.

qualitative point of view, this showed that the position of the NP luminescence peak was dependent on the conditions used for both the preparation and the analysis, such as the excitation wavelength, the APTS concentration, and the calcination temperature. The NP emission is red-shifted when the excitation is done at longer wavelengths or when the molar concentration of APTS increases (see Figure 3). This excitation-dependent emission phenomenon could be explained by the existence of discrete energy states within the energy gap after calcination. Transition between such states will depend on the excitation energy.¹⁶ In all cases, after calcination, higher emission intensities were observed to correlate with higher amounts of APTS used in the preparation. This trend was maintained up to 50% APTS, while higher amounts of APTS resulted in significant luminescence decay (see Figure 4). It is noteworthy that this was only observed for the particles heated above 600 °C. At 400 °C, the pattern was different. NPs containing the lowest amounts of APTS exhibited the highest luminescence signal, as shown in Figure 4. Furthermore, NP emission maxima shifted as a function of the calcination temperature. That is, the emission spectra ($\lambda_{\text{exc}} = 350$ nm) of NPs had a blue-shift when a higher heating temperature was used (700 °C compared to 600 °C in Figure 4).

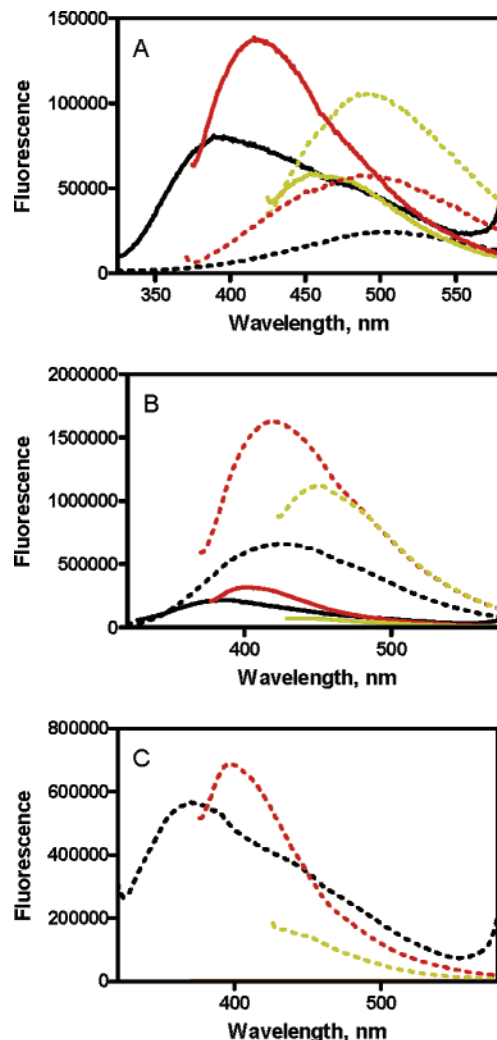


Figure 3. Influence of the excitation wavelength and the amount of organosilane (APTS) in the emission spectra. Calcination temperature: (A) 400 °C, (B) 600 °C, and (C) 700 °C. Lines: straight lines (—) 3% APTS and dashed lines (---), 50% APTS. Color code: black, $\lambda_{\text{exc}} = 300$ nm; red, $\lambda_{\text{exc}} = 350$ nm; and yellow, $\lambda_{\text{exc}} = 400$ nm.

More interestingly, after heating the APTS NPs at 600 and 700 °C, some of them also presented phosphorescence properties. For example, NPs incorporating 50% APTS and heated at 700 °C resulted in the emission of phosphorescence that persisted for more than 10 s, which was obvious to the naked eye after removing the irradiation light. This is consistent with previous results found for silicate glasses prepared under acidic conditions.⁷ In contrast, neither the NPs calcined at 400 °C nor the control samples (dye-doped NPs and pure silica NPs) exhibited phosphorescence. The phosphorescence of the NPs is particularly useful for time-resolved measurements to avoid background interference, scattering light, and autofluorescence of biological samples. In addition to APTS, other organosilane-incorporated NPs, for example, APTMS, 1-naphyltrimethoxysilane, phenyltriethoxysilane, or 1,4-bis(triethoxysilyl)benzene, could also emit phosphorescence after calcination at 600 and 700 °C. While the emission peak positions of these other organosilane-containing NPs were the same as those incorporating APTS, their absolute intensities were less. Lifetime measurements were performed for some of the NPs which showed clear phosphorescence using a spectrofluorometer with a double grating monochromator for both excitation and emission for highest stray light rejection. The fitting for the one-exponential model was not adequate

(16) Carlos, L. D.; de Zea Bermudez, V.; Sa Ferreira, R. A.; Marques, L.; Assuncao, M. *Chem. Mater.* **1999**, *11*, 581–588.

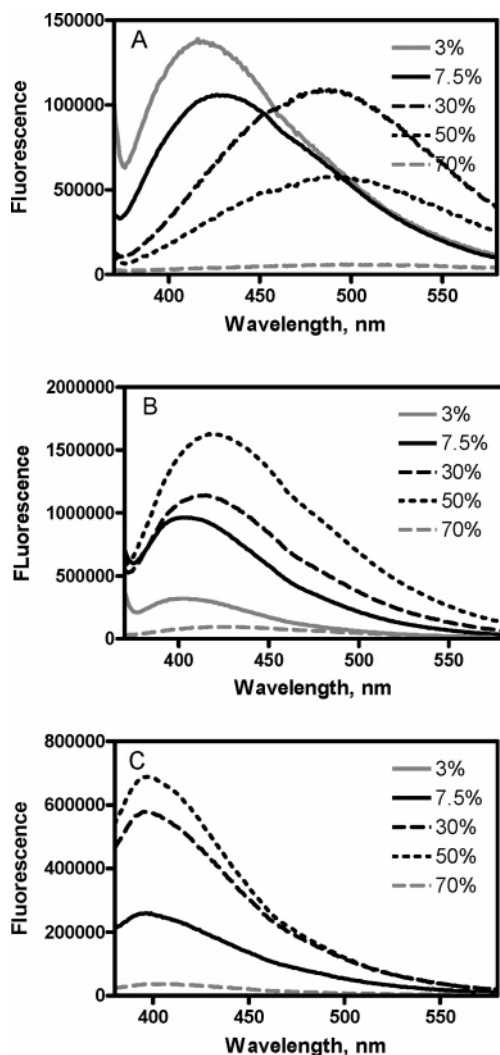


Figure 4. Influence of the amount of APTS on NP luminescence intensity. The excitation wavelength was 350 nm. Calcination temperature: (A) 400 °C, (B) 600 °C, and (C) 700 °C.

Table 2. Lifetime Data of NPs in Water^a

NP	y_0	A_1	t_1	A_2	t_2	R^2
50% APTS, 600 °C	219.91	377.247	2.678	532.759	0.318	0.9774
25% APTS, 700 °C	1647.87	2908.229	0.136	2009.906	1.198	0.9968
50% APTS, 700 °C	735.82	1665.317	0.303	1029.999	3.315	0.9900

^a Lifetime values (t) in milliseconds and relative amplitude values (A) corresponding to a two-exponential decay equation are listed. The excitation wavelength was 350 nm, and the emission wavelength was 414 nm, with an initial delay of 0.1 ms.

enough, and the curves were fitted to a double-exponential decay equation, as shown below:

$$Y = A_1 \exp(-x/t_1) + A_2 \exp(-x/t_2) + y_0$$

The lifetime data for three different NPs are summarized in Table 2. These data show lifetime values that are in the range of milliseconds, indicating a long-lived photoluminescence, likely phosphorescence. Those values are clearly longer than those for silica materials heated below 400 °C, which are in the range of nanoseconds,⁷ more according to fluorescence than phosphorescence.

The quantum yield (QY) of these NPs was determined by a comparative method¹⁷ with norharmane and quinine sulfate as standards; both of these compounds emit at a similar spectral region and possess a QY around 0.55. According to this method, to minimize reabsorption effects, the concentrations of both the standards and the nanoparticles were selected to give an absorbance value below 0.1 U.A. at and above the excitation wavelength when using a 10 mm path length cuvette. Above this level, nonlinear effects may be observed due to inner filter effects, resulting in perturbed quantum yield values. The QY value determined for the NPs was low (around 0.05), which indicates that these particles are still far from the brightness achieved using dye-doped NPs.

The stability of the particles in terms of luminescent properties was also studied. It was found that the photoluminescence emission from the NPs is quite stable and shows no diminishing effects after exposure to the ambient environment for more than 6 months. These particles also showed the same emission profiles when dried or dissolved in a variety of conditions such as acidic, basic, aprotic, polar, and hydrophobic solvents (data not shown), indicating that the chromophore responsible for the luminescence is trapped inside the spheres.

To better understand the mechanisms underlying NP luminescence and nanostructure changes, elemental analysis was performed on the 30% APTS NPs before and after calcination at different temperatures. It was found that, after calcination, the C, H, and N weight percentages in the silica NPs were reduced. The C content decreased from 6.08% to 1.79% after heating at 400 °C and then gradually to 0.75%, 0.28%, and 0.25% when calcined at 600, 700, and 800 °C, respectively. Similarly, the weight percentage of N and H decreased from 2.54% and 2.85% to 0.21% and 0.86%, respectively, after heating at 400 °C. Thus, higher temperature led to more loss of C, H, and N until a percentage close to zero was reached. It is known that SiO₂ has a high-energy band gap (5.4 eV). With various impurities introduced into the silica network, such as C, Sn, or excess O, defect excited states are generated, and the band gap can be decreased, which makes the interaction with visible light possible.^{18–20} The presence of chemical groups with electron-donating ability within the light-generating nanoclusters, such as amine groups, will therefore be a favorable factor for making an efficient photoluminescent particle. Based on this evidence, it is reasonable to assume that the NP photoluminescence emission can be obtained when C- and/or OH-based species are intentionally introduced into the silica NPs. In addition, when silica NPs doped with organosilane “impurities” are heat-treated at various temperatures, the changes in the molecular structure and the surrounding environment may result in different electronic transitions, causing, in turn, the different optical properties exhibited by the NPs. The lack of luminescence in particles heated at 800 °C could then be attributed to the degradation of the organic (carbon centers) impurities introduced to the silica matrix, leading to the suppression of the photoluminescence properties. We believe that further clarification of the conditions for the luminescence emission will lead to the production of NPs with even greater efficiency in visible light emission.

(17) Williams, A. T. R.; Winfield, S. A.; Miller, J. N. *Analyst* **1983**, *108*, 1067–71.

(18) Chiodini, N.; Meinardi, F.; Morazzoni, F.; Paleari, A.; Scotti, R.; Di Martino, D. *J. Non-Cryst. Solids* **2000**, *261*, 1–8.

(19) Sakurai, Y.; Nagasawa, K. *J. Non-Cryst. Solids* **2000**, *261*, 21–27.

(20) Sendova-Vassileva, M.; Tzenov, N.; Dimova-Malinovska, D.; Marinova, T.; Krastev, V. *Thin Solid Films* **1996**, *276*, 318–322.

Conclusions

In this work, luminescent, stable, cost-effective, and nontoxic silica NPs were prepared using the Stöber synthesis method and the microemulsion method. After heating at different temperatures, the NPs became luminescent. After calcination at 600 or 700 °C, the particles generated a phosphorescence signal. It seems clear that several factors such as the type and quantity of organosilane, calcination temperature, and excitation wavelength all affect particle luminescence properties, indicating that a complex mechanism might be involved in the generation of luminescence. The photoluminescence emission from the NP samples is quite stable and shows no aging effects after exposure to the ambient environment for more than 6 months. In addition, by heating the NPs at 600 or 700 °C, the NPs gave a phosphorescent afterglow after UV illumination. Despite the current low quantum yield, these particles show promise as an alternative for probes by taking advantage of the long lifetime phosphorescence property. Since their long lifetime permits time-resolved measurements to avoid background interference, scat-

tering light, and autofluorescence, the phosphorescence signal of these NPs makes them promising for bioassays. Finally, these NPs may also hold great promise for optical display as an alternative type of phosphor material. One possible explanation for the luminescence of these NPs is the carbon/oxygen-related defect center mechanism resulting from calcination of the organosilane-containing spheres. However, more studies are needed to understand the underlying luminescent mechanism.

Acknowledgment. We thank Dr. Lin Chandler for performing the lifetime measurements of the nanomaterials. This work was supported by the NIH, State of Florida Center of Excellence, and ONR Grant. L.W. acknowledges support as an ACS Division of Analytical Chemistry Fellow sponsored by GlaxoSmithKline. M.-C.E. acknowledges financial support from the Departament d'Universitats, Recerca i Societat de la Informació de la Generalitat de Catalunya, Spain.

LA703392M